

CONFERENCES AND SYMPOSIA

PACS number: 01.10.Fv

Joint scientific session of the Physical Sciences Division of the Russian Academy of Sciences and the Joint Physical Society of the Russian Federation (16 April 2003)

A joint scientific session of the Physical Sciences Division of the Russian Academy of Sciences (RAS) and the Joint Physical Society of the Russian Federation was held on 16 April 2003 at the P N Lebedev Physics Institute, RAS. The following reports were presented at the session:

(1) **Rozanov V B** (P N Lebedev Physics Institute, RAS, Moscow) "On the possibility of the spherical compression of laser fusion targets using two-beam irradiation";

(2) **Kulakovskiĭ V D, Krizhanovskiĭ D N, Tartakovskiĭ A I** (Institute of Solid State Physics, RAS, Chernogolovka), **Gippius N A, Tikhodeev S G** (General Physics Institute, RAS, Moscow) "Polariton – polariton scattering and the nonequilibrium condensation of exciton polaritons in semiconductor microcavities";

(3) **Sibel'din N N** (P N Lebedev Physics Institute, RAS, Moscow) "Magnetically stabilized multiparticle bound states in semiconductors";

(4) **Klimov V V** (P N Lebedev Physics Institute, RAS, Moscow) "Spontaneous atomic radiation in the presence of nanobodies";

(5) **Volkov B A** (P N Lebedev Physics Institute, RAS, Moscow) "Electronic properties of narrow gap IV – VI semiconductors";

(6) **Belyanin A A** (Institute of Applied Physics, RAS, Nizhniĭ Novgorod; Institute for Quantum Studies and Department of Physics, Texas A&M University, College Station, Texas, USA), **Deppe D** (Department of Electrical and Computer Engineering, University of Texas, Austin, USA), **Kocharovskiĭ V V** (Institute of Applied Physics, RAS, Nizhniĭ Novgorod; Institute for Quantum Studies and Department of Physics, Texas A&M University, College Station, Texas, USA), **Kocharovskiĭ Vl V** (Institute of Applied Physics, RAS, Nizhniĭ Novgorod), **Pestov D S** (Institute of Applied Physics, RAS, Nizhniĭ Novgorod; Institute for Quantum Studies and Department of Physics, Texas A&M University, College Station, Texas, USA), **Scully M O** (Institute for Quantum Studies and Department of Physics, Texas A&M University, College Station, Texas, USA) "New semiconductor laser designs and the exploratory investigation of the terahertz frequency range";

(7) **Semenov V E** (Institute of Applied Physics, RAS, Nizhniĭ Novgorod) "Dynamics of plasma bunches in external fields";

(8) **Molotkov S N** (Institute of Solid State Physics, RAS, Chernogolovka) "Quantum cryptography: on the way to unconditional secrecy".

An abridged version of the reports 2 – 6 is given below.

Uspekhi Fizicheskikh Nauk **173** (9) 995 – 1021 (2003)
Translated by E G Strel'chenko, M V Chekhova, E N Ragozin; edited by A Radzig

PACS numbers: **71.36.+c**, **78.67.–n**
DOI: 10.1070/PU2003v046n09ABEH001626

Polariton – polariton scattering and the nonequilibrium condensation of exciton polaritons in semiconductor microcavities

V D Kulakovskiĭ, D N Krizhanovskiĭ, A I Tartakovskiĭ, N A Gippius, S G Tikhodeev

Semiconductor microcavities (MCs) with quantum wells (QWs) in the active layer provide a system of particular interest for the study of mixed exciton – photon states [1]. Such states — which have come to be known as microcavity polaritons — are realized when the damping of both the photon and exciton modes does not exceed the exciton – photon interaction energy. The dispersion of MC polaritons is determined by two parameters: the energy mismatch $\delta = E_C - E_X$ between the exciton and photon modes at point $\mathbf{k} = 0$, and the exciton – photon coupling Ω. In the strong exciton – photon coupling regime, the exciton and photon modes undergo mutual repulsion giving rise to two — upper and lower — polariton branches. The formation of MC polaritons is illustrated in Fig. 1.

In flat microcavities, polaritons are the quasi-two-dimensional particles. Unlike polaritons in bulk semiconductors, MC polaritons annihilate without conserving momentum in the direction perpendicular to the plane of the quantum well, which leads to short — picosecond — lifetimes. On the other hand, the effective mass of MC polaritons turns out to be several orders of magnitude lower than that of excitons, and their coherence length exceeds several microns: these two factors change the properties of the exciton system qualitatively [1 – 3]. In recent years it has been found, in particular, that the exciton – polariton system exhibits strong nonlinearities in radiation intensity and polarization at large energy densities of resonant excitation [2, 3].

Strong nonlinearities in MC luminescence have been observed [4 – 10] under resonant excitation of the lower polariton branch (LPB) with the horizontal momentum projection $\mathbf{k}_p$ close to the inflection point of the LPB dispersion curve. The effect is explained by the four-wave

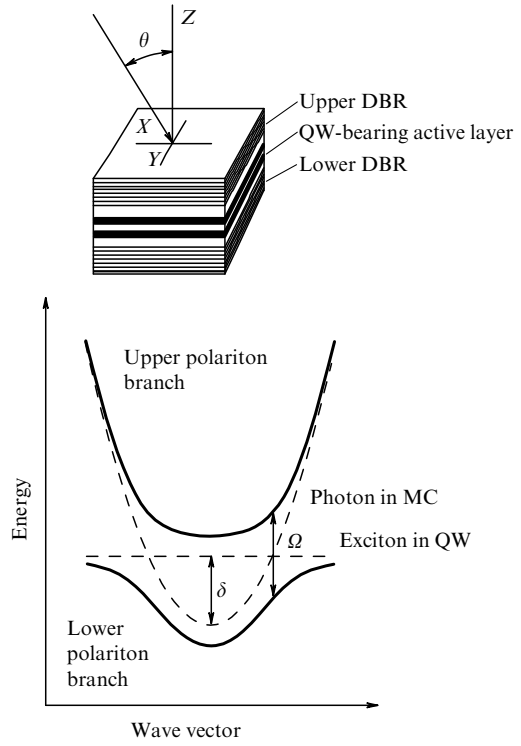

Figure 1. The formation of the upper and lower polariton branches (solid lines) in a microcavity. Dashed lines correspond to photon dispersion in the empty microcavity, and to exciton dispersion in a quantum well. The schematic structure of the microcavity and the geometry of the experiment are shown in the inset to the figure.

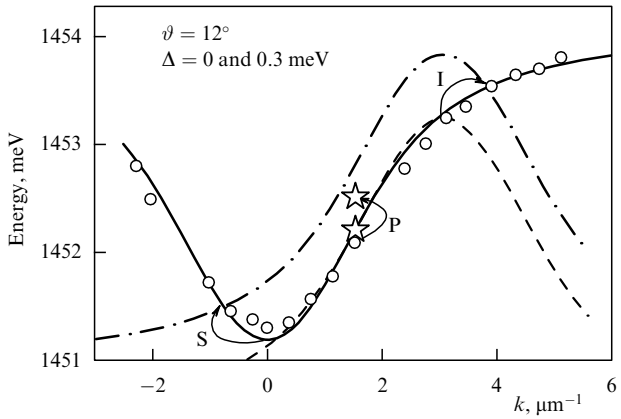

Figure 2. Lower polariton branch $E_{LP}(\mathbf{k})$ in a microcavity. Circles correspond to experimental data, the solid line to calculations, and the stars to pumping (P) at angle $\vartheta_p = 12°$ (at the inflection point of the LPB) and to mismatches $\Delta = E_p - E_{LP}(\mathbf{k}_p) \approx 0$ and ~ 0.3 meV. Dot-and-dash and dashed lines present the dependences $2E_p - E_{LP}(2\mathbf{k}_p - \mathbf{k})$ obtained for $\Delta \approx 0$ and $\Delta \approx 0.3$ meV, respectively. The points of intersection of the solid with the dot-and-dash and dashed lines determine the energies and momenta of the scattered polaritons — the signal (S) and idle (I) — in the four-wave-mixing model. Arrows indicate the expected direction of the shift for S and I on going over from resonant excitation at LPB inflection point $\Delta \approx 0$ to $\Delta \approx 0.3$ meV.

mixing or parametric scattering of photoexcited polaritons, which occurs from the state $(E_p, \mathbf{k}_p)$ with the energy E_p and momentum $\mathbf{k}_p$ to the 'signal' (S) state $(E_s, \mathbf{k}_s)$ and 'idle' (I) state $(E_i, \mathbf{k}_i)$ and which conserves energy and quasi-momentum, i.e., one has

$$\mathbf{k}_s + \mathbf{k}_i = 2\mathbf{k}_p\,, \qquad E_s + E_i = 2E_p\,. \tag{1}$$

The conversion coefficient reaches 10%, making MC structures very promising for polariton thresholdless lasers [10].

To describe the effects observed, the four-wave-mixing model [2, 4, 6, 7] is employed; the model was developed for describing a system with a single macrofilled mode $(E_p, \mathbf{k}_p)$, and it is explained in Fig. 2. It is seen from the figure that under excitation one can satisfy the energy and momentum conservation laws for $\mathbf{k}_s \approx 0$ and $\mathbf{k}_i \approx 2\mathbf{k}_p$ at the inflection point [4]. The theory of four-wave mixing suggests that a change in the excitation angle (i.e., $\mathbf{k}_p$) or in the energy E_p of the exciting laser should lead to changes in E_s, E_i, $\mathbf{k}_s$, and $\mathbf{k}_i$ because the scattering should culminate in transitions to the allowed LPB states with $\mathbf{k}$'s satisfying the conservation laws (1). The expected behavior is illustrated in Fig. 2. We found, however, that for excitation densities above a certain critical value, changes in E_p or $\mathbf{k}_p$ lead to surprising results: the scattering always brings about the occupation of states with $\mathbf{k}_s \approx 0$, and $E_s(\mathbf{k}_s)$ and $E_i(\mathbf{k}_i)$ turn out to be far above the polariton branch. Below we will examine the possible causes of such a behavior.

Our experiments examined polariton – polariton scattering in a GaAs-based MC semiconductor structure (see inset to Fig. 1). The structure incorporates distributed Bragg reflectors (DBRs) made of $\lambda/4$-thick repetitive layers of $Al_{0.13}Ga_{0.87}As/AlAs$ (17 layers in the front and 20 in the rare reflectors) and contains an active layer with InGaAs quantum wells. The structure was grown by molecular-beam epitaxy on a GaAs substrate ~ 0.5 mm in thickness. In the MC's active layer consisting of the GaAs material $3\lambda/2$ thick, six $In_{0.06}Ga_{0.94}As/GaAs$ quantum wells 10 nm thick were placed. The Rabi splitting Ω amounted to ≈ 6 meV. The MC was grown in such a way that the thickness of its active layer varied smoothly along the sample. This leads to a change in the photon mode energy E_C and, accordingly, in the mismatch between the exciton energy E_X and the photon mode energy in the states with $\mathbf{k} = 0$. Sample regions with $\delta = 1$ and -1.5 meV were investigated in the experiments.

The resonant photoexcitation of polaritons was achieved with a solid-state continuous titan-sapphire (TiSP) laser, and nonresonant above-gap excitation with an HeNe laser. The sample was placed in a helium cryostat where the temperature was varied from 5 to 15 K by a thermoregulation system accurate to within ~ 0.05 K. Photoluminescence (PL) was collected at various angles using lenses and an optical fiber, all mounted on a goniometer arm. Angular resolution was achieved by a diaphragm controlling a solid angle of $\sim 0.5°$. To register the PL signal, a 1-m double monochromator and nitrogen-cooled CCD camera were used.

By employing high angular resolution spectroscopy and independently choosing the photoexcitation and observation angles it is possible to resonantly excite polaritons with a fixed quasi-momentum and to measure polariton distribution in momentum space. Because the tangential component of the light momentum is conserved at the vacuum – MC boundary, the polariton quasi-momentum $\mathbf{k}$ and the angle of incidence ϑ are related by the simple expression $k = |\mathbf{k}| = (E/c)\sin\vartheta$. Because the work was done under continuous excitation conditions, both the momentum and the energy of polaritons were determined with high accuracy.

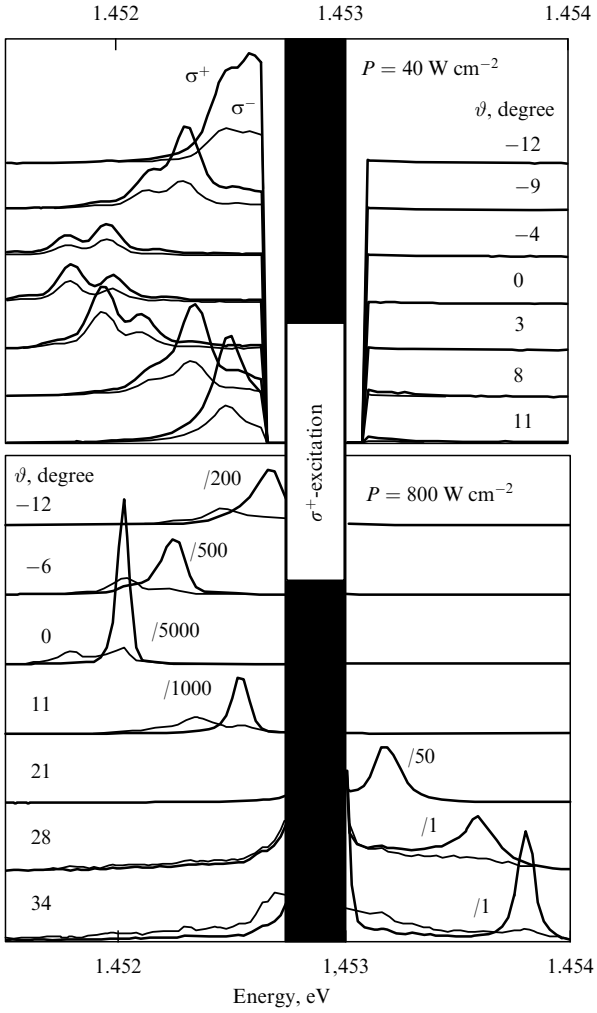

Figure 3. Angular dependence of MC emission spectra for weak and strong resonant σ^+-photoexcitation, recorded for two polarizations. The black vertical strip corresponds to the pumping strip where photoluminescence was not measured.

Figure 3 shows MC emission spectra for the LPB excited resonantly by σ^+-polarized light. For weak excitation, the intensity and the degree of polarization of the emission line decrease with the approach to the bottom of the LPB band, the transition energies being the same for the σ^+ and σ^- polarizations. As the excitation density is increased, the σ^- spectra remain unchanged, whereas the σ^+-polarized emission line is shifted to the violet and strongly narrowed in the vicinity of $\mathbf{k} = 0$, its intensity growing exponentially with excitation density. As a result, the emission becomes almost 100% σ^+-polarized at high excitation densities. Simultaneously, an idle parametric scattering signal I emerges on the quasi-momentum $2\mathbf{k}_p$, which is located above the excitation energy in accordance with Eqn (1). The appearance of line I in the spectrum shows that parametric scattering does make a significant contribution, and the exponential growth testifies to the self-stimulated nature of the scattering. Such a regime occurs when the occupation of states near $\mathbf{k} = 0$ turns out to be more than unity, and scattering into these states is further stimulated by the boson nature of polaritons. A lower estimate of the filling factors of the states contributing to the S line can be obtained using the polariton lifetime and the measured S signal emission power density. In the MC studied, the polariton emission time is determined by the DBRs and ranges from 3 to 5 ps. The lateral dimension of the MC's emitting region virtually coincides with the photoexcitation region and is equal to ~ 50 μm. For the excitation power density of 100 mW cm^{-2}, the stationary number of polaritons reaches 10^4. Measurements of the S-line emission angular distribution show that this number of polaritons falls in the range of the quasi-momenta $\mathbf{k}$ that do not exceed 5×10^3 cm^{-1}. Thus we see that the average mode occupation number is not less than 10.

The signal behavior under the variation of the frequency of the exciting laser light for a fixed excitation angle is strongly dependent on whether the frequency E_p shifts to above or below the polariton branch. In the latter case, the threshold for stimulated scattering sharply increases and exceeds 1000 W cm^{-2} already for a mismatch of -0.5 meV. As the laser frequency is increased above the LPB, the threshold power for stimulated scattering grows much more weakly. Moreover, as discussed below, under certain conditions an increase in E_p above the LPB at first even leads to a marked decrease of P_{th}, and it turns out, unexpectedly, that for all E_p the values of $\mathbf{k}_s$ and $\mathbf{k}_i$ remain virtually unchanged and that the S and I lines shift to energies well above the lower polariton branch. The positions of the maxima of the S and I peaks for a number of values of E_p ($\mathbf{k}_p = 1.9 \times 10^4$ cm^{-1}) is shown in Fig. 3. If the S line remained on the polariton branch, then, by the law of conservation of energy, E_i should shift from the polariton branch twice as fast as E_p toward higher energies. However, it is seen from the figure that the energy conservation law is fulfilled because both E_s and E_i increase, the departures of E_s and E_i from the LPB being comparable. This behavior differs qualitatively from that expected from the standard four-wave-mixing model.

The measured E_p-dependences of the MC absorption coefficients, LPB emission intensity, and the spectral position of the LPB emission line are depicted in Figs 4a–c, respectively, for a fixed excitation angle of $\sim 14°$ ($\mathbf{k}_p = 1.9 \times 10^4$ cm^{-1}) provided by a TiSP laser. All the dependences for the MC with $\delta \approx -1.5$ meV are recorded for $T = 5.2$ K and two different excitation conditions (a TiSP laser alone or together with an HeNe laser).

From the comparison of the three figures it is seen that under excitation below the stimulated parametric scattering threshold the absorption maximum of the exciting laser radiation coincides with the energy position of the polariton branch and, as expected, the emission maximum is also observed for resonant excitation in the LPB. An additional weak above-gap excitation (no more than 10% of the resonant excitation) produces stimulated parametric scattering in the polariton system. While this leaves the MC's absorption peak unshifted, the maximum signal is now observed not for the resonant excitation in the LPB, where the MC absorption peak is positioned, but for excitation to 1 meV above the LPB. We can conclude therefore that the density of photoexcited polaritons does not determine the development of stimulated parametric scattering.

In order to simulate the process of parametric scattering of polaritons, the following system of equations was solved numerically for $\mathcal{E}_{QW}$, the QW electric field, and $\mathcal{P}(k,t)$, the QW-width-averaged exciton polarization:

$$\left[\mathrm{i}\,\frac{\mathrm{d}}{\mathrm{d}t} - E_C(k)\right]\mathcal{E}_{QW}(k,t) = \alpha(k)\mathcal{E}_{ext}(k,t) + \beta(k)\mathcal{P}(k,t)\,, \tag{2}$$

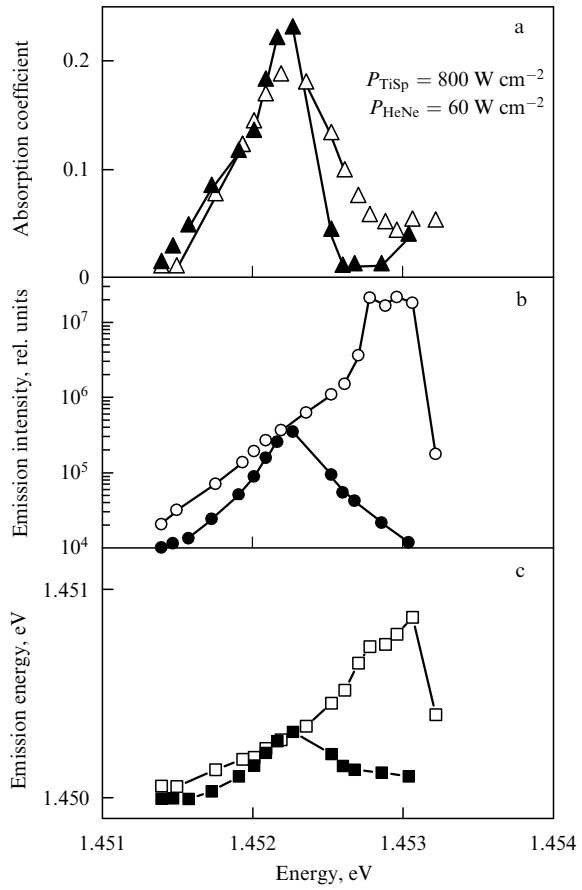

Figure 4. MC absorption coefficient (a), LPB emission intensity (b), and the spectral position of the emission line (c) as functions of the resonant excitation energy on irradiation by a TiSP laser alone (▲, ●, ■) and in combination with an HeNe laser (Δ, ○, □).

$$\left[\mathrm{i}\frac{\mathrm{d}}{\mathrm{d}t} - E_X\right]\mathcal{P}(k,t) = F\sum_{q,q'}\mathcal{P}(q,t)\,\mathcal{P}(q',t)\mathcal{P}^*(q+q'-k,t) + A\mathcal{E}_{QW}(k,t) + \xi(k,t)\,. \qquad (3)$$

Here, the electric field $\mathcal{E}_{ext}(k,t) = \mathcal{E}(t)\exp(-\mathrm{i}E_p t)\,\delta(k-k_p)$ of the incident electromagnetic pumping wave far away from the MC is described by a macrofilled photon mode with a fixed frequency E_p, wave number $k_p = E_p \sin\vartheta/c$, and time-variable amplitude $\mathcal{E}(t)$; E_C, E_X is the resonant frequency of an empty MC and the exciton frequency in a free QW, respectively; F is the exciton–exciton coupling constant; A is the exciton polarizability, and $\xi(k,t)$ is the Langevin random force, for which $\langle\xi(k,t)\rangle = 0$ and $\langle\xi(k,t)\,\xi(k',t')\rangle = \Xi\delta(k-k')\,\delta(t-t')$. The MC response constants α and β are calculated using the scattering matrices of the upper and lower DBRs for $\omega = E_C(k)$. For simplicity, instead of the original quasi-two-dimensional problem, a spatially one-dimensional problem is considered.

Equation (2) is the Maxwell equation accounting for exciton polarization and is written in the resonant scalar approximation, the term scalar meaning that the $\sigma^{\pm}$ polarizations are not allowed to mix. Equation (3) constitutes an inhomogeneous nonlinear Schrödinger equation for exciton polarization and includes two types of sources: a coherent external excitation and a stochastic Langevin noise. The latter makes it possible to model the quantum fluctuations of the scattering signal when using quasi-classical equations (2) and (3).

The nonlinear Schrödinger equation takes into account only the contact exciton–exciton interaction. The model does not include, for example, the exciton–phonon coupling which may play a very important role in how the parametric scattering of MC polaritons occurs. However, even in this simplest approximation the model turns out to exhibit a threshold behavior in a certain range of parameters, which is qualitatively similar to that observed in experiment. As the pumping intensity is increased, the numerical solutions of the system of equations (2)–(3) demonstrate [11] an abrupt passage from the classical four-wave-mixing picture — in which, in accordance with the theory, the scattered polariton signals S and I are located on the blue-shifted LPB — to a situation in which the signal is observed at $k_s \approx 0$, and idle polaritons at $k_i \approx 2k_p$ independent of the mismatch Δ and the excitation angle ϑ_p.

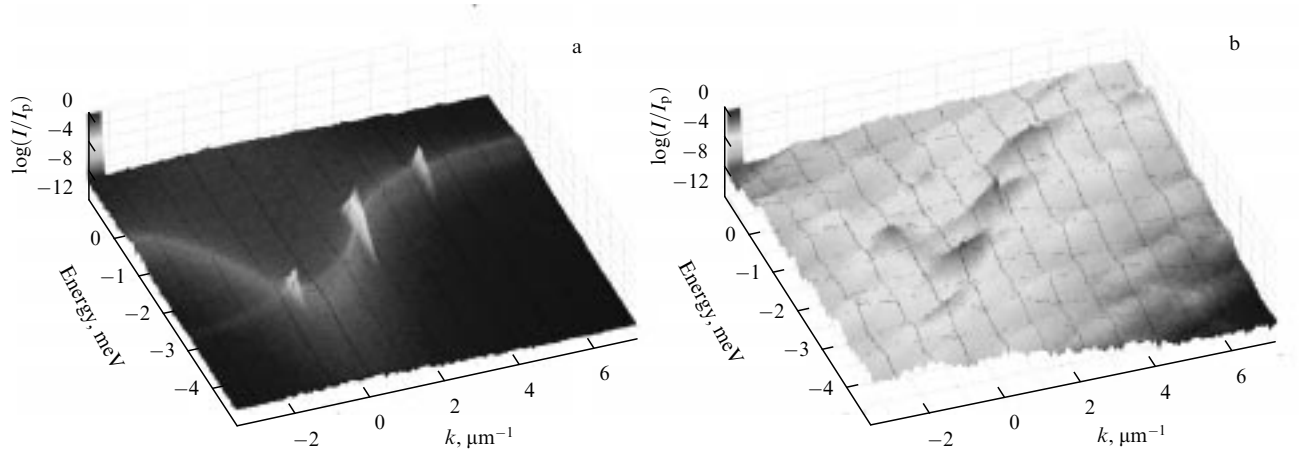

Figure 5. Theoretically evaluated energy and wave-number distributions of polaritons for pumping (a) below, 99%, and (b) above, 101%, threshold P_{th}. Energy is reckoned from $E_C(k=0)$. The relative intensity of scattered polaritons (normalized to the pumping intensity) is plotted along the vertical on a logarithmic scale and is also shown by shades of gray (see the vertical scale). Note that the average intensity of the scattered polariton noise grows by five to six orders of magnitude after the threshold, which corresponds to the general background changing from black to gray in figures (a) and (b), respectively. The exciting wave in both the figures is detuned by $E_p - E_{LP} = 0.3$ meV from the LPB and is incident at an angle of 14° corresponding to the momentum $k_p \approx 1.9$ μm^{-1}.

The passage involves an increase in the intensity of the scattered polariton signal by many orders of magnitude and is illustrated in Fig. 5. In numerical simulations, the pumping amplitude $\mathcal{E}(t)$ was first switched on at 99% of its maximum for about 100 ps, then increased slowly to the maximum value for $\sim$ 1000 ps, and then switched off within another 100 ps.

The physical mechanism of the above passage is due to the fact that the decay of a pumping polariton to the S and I polaritons becomes parametrically unstable when a certain critical pumping intensity is reached, and due to the presence of an absolutely unstable negative slope region on the S-like plot showing the way the exciton polarization $\mathcal{P}(k_p, t)$ at the pumping angle varies with pumping amplitude. The parametric decay instability is similar to that in Ref. [12] discussing the Mandelstam – Brillouin scattering of an intense polariton wave. It is only this type of instability which was considered in the previous analyses [6, 8 – 10] of the parametric scattering of MC polaritons. Our calculations show, however, that due to the development of parametric scattering instability, the response of a nonlinear oscillator at the pumping angle may become unstable during the actual evolution of a system. As a result, instead of the parametric build-up of macrofilled modes for $k_s \neq 0$ and $k_i \neq 2k_p$, the spectrum of the scattered polariton signal is strongly rearranged, acquiring maxima at $k_s \approx 0$ and $k_i \approx 2k_p$, and an increase by several orders of magnitude in the total scattered intensity is observed. This behavior is qualitatively consistent with that observed in experiment.

Acknowledgments. The authors are grateful to L V Keldysh for numerous discussions, and M Skolnik for providing the samples. Partial financial support from the RFBR and INTAS is gratefully acknowledged.

References

1. Weisbuch C et al. *Phys. Rev. Lett.* **69** 3314 (1992)
2. Baumberg J J et al. *Phys. Rev. B* **62** R16247 (2000)
3. Kulakovskiĭ V D et al. *Usp. Fiz. Nauk* **170** 912 (2001) [*Phys. Usp.* **43** 853 (2001)]
4. Stevenson R M et al. *Phys. Rev. Lett.* **85** 3680 (2000)
5. Tartakovskii A I, Krizhanovskii D N, Kulakovskii V D *Phys. Rev. B* **62** R13298 (2000)
6. Savvidis P G et al. *Phys. Rev. Lett.* **84** 1547 (2000)
7. Ciuti C et al. *Phys. Rev. B* **62** R4825 (2000)
8. Ciuti C, Schwendimann P, Quattropani A *Phys. Rev. B* **63** 041303(R) (2001)
9. Savvidis P G et al. *Phys. Rev. B* **64** 075311 (2001)
10. Saba M et al. *Nature* **414** 731 (2001)
11. Gippius N et al., in *Proc. of the 26th Intern. Conf. on the Physics of Semiconductors, 29 July – 2 Aug. 2002, Edinburgh, UK* (London: IOP, 2002) p. G4-6
12. Keldysh L V, Tikhodeev S G *Zh. Eksp. Teor. Fiz.* **90** 1852 (1986) [*Sov. Phys. JETP* **63** 1086 (1986)]

PACS numbers: 71.35.Ee, 71.35.Ji

DOI: 10.1070/PU2003v046n09ABEH001644

Magnetically stabilized multiparticle bound states in semiconductors

N N Sibel'din

1. Introduction

Under laboratory conditions, a magnetic field acting on an atom removes the degeneracy with respect to the directions of the angular momentum (Zeeman and Paschen – Back effects) and causes a slight diamagnetic shift of the high-lying energy levels; however, the inner structure of the atom (electron density distribution) and its energy spectrum (neglecting the splitting of the levels in a magnetic field, which is small compared to the atomic electron binding energy) remain virtually unchanged. The effect of a magnetic field becomes significant when the field strength is sufficiently large, such that the cyclotron energy of a free electron, $\hbar\omega_c = \hbar eH/cm$, where m is the electron mass, becomes comparable to the electron binding energy in the atom, and the magnetic length $a_H = \sqrt{c\hbar/eH}$ is of the order of the atomic radius. In the case of the hydrogen atom, for example, this implies the field strength $H \sim 10^9$ Oe, which is beyond the reach of modern experiments. We therefore depend on astrophysical observations or experiments on model systems when wish to draw information on the properties of atoms in strong magnetic fields.

The most attractive objects for such studies are apparently excitons and the atoms of hydrogen-like impurities in semiconductors. The ground-state energy and the Bohr radius of an exciton (an atom of a hydrogen-like impurity) in a semiconductor crystal are given by the Bohr formulas, which in this case take the form

$$E_{ex} = -\frac{m^* e^4}{2\varkappa^2\hbar^2}\,, \tag{1}$$

$$a_{ex} = \frac{\varkappa\hbar^2}{m^* e^2}\,, \tag{2}$$

where $\varkappa$ is the dielectric constant of the crystal, and m^* is the reduced effective mass of an electron and a hole (the effective mass of an electron or a hole for shallow donors and acceptors, respectively). Due to the large dielectric constant of the medium and because of the small effective masses of the electrons and holes, the binding energies of excitons, $|E_{ex}|$, and of hydrogen-like impurities are typically 3 to 4 orders of magnitude smaller than for the hydrogen atom, and their Bohr radii 2 to 3 orders of magnitude larger. In the fields of equal strength, the cyclotron frequency of charge carriers in a semiconductor is m/m^* times that of a free electron, making even $H \sim 10^3 - 10^4$ Oe a strong field for excitons and the atoms of shallow impurities.

The behavior of hydrogen-like impurities in strong magnetic fields was treated theoretically in Refs [1 – 3], and the bebavior of excitons in Refs [4 – 6]. A magnetic field stabilizes excitonic (atomic) states. In weak fields, the binding energy increases because the free-electron energy (the cyclotron frequency) increases linearly with the field strength, whereas that of a bound electron in an atom increases quadratically (diamagnetic shift). In ultrahigh fields ($\hbar\omega_c \gg |E_{ex}|$), the centripetal force acting on an electron orbiting the nucleus in the plane perpendicular to the magnetic field direction is dominated by the Lorentz force (the Coulomb interaction of the electron with the nucleus — or with a hole in an exciton — can be treated as a perturbation). An exciton (atom) is strongly anisotropic; its shape is an ellipsoid of revolution oriented along the magnetic field, with semi-axes a_{ex} and a_H in the longitudinal and transverse directions, respectively. The exciton binding energy $|E_{ex}|$ increases in proportion to $\ln^2 H$ as the field strength is increased [6]. Such excitons were called diamagnetic [7].

Experimentally, effects related to the increase in the ionization energy of shallow donors in a magnetic field were first observed in heavily doped indium antimonide (magnetic